DOI: 10.1002/cmdc.200700194

Inhibition of HIV-1 by a Peptide Ligand of the Genomic RNA Packaging Signal Ψ

Julia Dietz,[a] Joachim Koch,[b] Ajit Kaur,[c] Chinnappan Raja,[d] Stefan Stein,[a] Manuel Grez,[a] Anette Pustowka,[a] Sarah Mensch,[c] Jan Ferner,[c] Lars Möller,[e] Norbert Bannert,[e] Robert Tampé,[b] Gilles Divita,[f] Yves Mély,[d] Harald Schwalbe,*[c] and Ursula Dietrich*[a]

The interaction of the nucleocapsid NCp7 of the human immunodeficiency virus type 1 (HIV-1) Gag polyprotein with the RNA packaging signal Ψ ensures specific encapsidation of the dimeric full length viral genome into nascent virus particles. Being an essential step in the HIV-1 replication cycle, specific genome encapsidation represents a promising target for therapeutic intervention. We previously selected peptides binding to HIV-1 Ψ-RNA or stem loops (SL) thereof by phage display. Herein, we describe synthesis of peptide variants of the consensus HWWPWW motif on membrane supports to optimize Ψ-RNA binding. The optimized peptide, psi-pepB*, was characterized in detail with respect to its conformation and binding properties for the SL3 of the Ψ packaging signal by NMR and tryptophan fluorescence quenching. Functional analysis revealed that* psi-pepB *caused a strong reduction of virus release by infected cells as monitored by reduced transduction efficiencies, capsid p24 antigen levels, and electron microscopy. Thus, this peptide shows antiviral activity and could serve as a lead compound to develop new drugs targeting HIV-1.*

Introduction

During HIV-1 assembly the viral genome is efficiently encapsidated over cytoplasmic mRNA because of the specific recognition of the highly structured RNA packaging signal Ψ by the two zinc fingers of the viral NCp7 domain of the Gag polyprotein precursor (Figure 1). The Ψ-region consists of four stem loops, SL1 to SL4, within the 5′ UTR of the unspliced HIV-1 RNAs.[2–5] High affinity binding of aromatic and hydrophobic amino acids of the NC zinc fingers to SL2 and the major packaging signal SL3, in particular tryptophan W37 to the GGAG tetraloop, is followed by less specific interactions of basic amino acids in NCp7 leading to the co-assembly of Gag with the genomic RNA in the form of a dimeric molecule.[2–6] As genomic RNA encapsidation is essential for HIV-1 replication, disruption of the specific interaction between Ψ-RNA and NCp7 zinc fingers should interfere with virus production. Indeed, Zn^{2+} ejection, application of antisense RNA against Ψ-RNA elements or Ψ-RNA decoys resulted in antiviral activity in vitro.[7–13]

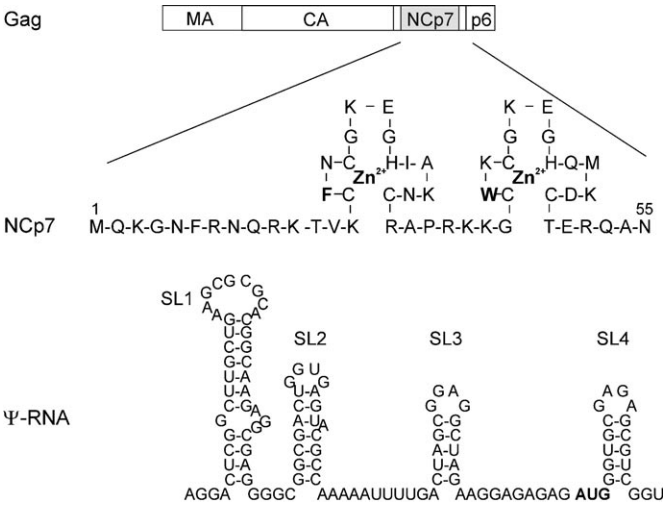

Figure 1. The nucleocapsid domain NCp7 of HIV-1 Gag interacts with the Ψ-RNA structure. Aromatic amino acids within the zinc fingers of NCp7 (bold) interact with Ψ-RNA, in particular with the GGAG tetraloop of SL3.

[a] *J. Dietz,[+] Dr. S. Stein, Dr. M. Grez, Dr. A. Pustowka, Dr. U. Dietrich*
Georg-Speyer-Haus, Institute for Biomedical Research
Paul-Ehrlich-Str. 42-44, 60596 Frankfurt (Germany)
Fax: (+49) 69 6339 5297
E-mail: ursula.dietrich@em.uni-frankfurt.de

[b] *Dr. J. Koch,[+] Prof. Dr. R. Tampé*
Institute of Biochemistry
Johann Wolfgang Goethe-University Frankfurt (Germany)

[c] *A. Kaur, S. Mensch, J. Ferner, Prof. Dr. H. Schwalbe*
Institute for Organic Chemistry and Chemical Biology
Center for Biomolecular Magnetic Resonance
Johann Wolfgang Goethe-University Frankfurt
Max-von-Laue-Str. 9, 60438 Frankfurt (Germany)
Fax: (+49) 69 798 29515
E-mail: schwalbe@nmr.uni-frankfurt.de

[d] *Dr. C. Raja, Prof. Dr. Y. Mély*
Département Pharmacologie et Physicochimie
Faculté de Pharmacie, Institut Gilbert-Laustriat
UMR 7175 CNRS/Université Louis Pasteur

[e] *L. Möller, Dr. N. Bannert*
Center for Biological Safety 4, Robert Koch Institute

[f] *Dr. G. Divita*
Centre de Recherches de Biochimie Macromoleculaires
CRBM-CNRS

[+] *These authors contributed equally to this work.*

Supporting information for this article is available on the WWW under http://www.chemmedchem.org or from the author.

We and others selected peptide ligands for Ψ-RNA from phage displayed peptide libraries to interfere with NCp7 binding.[1,14] Interestingly, the selected peptides were rich in tryptophans and these amino acids were important for binding to Ψ-RNA, such as W37 in the natural ligand NCp7 (Figure 1). Although the selected peptides interacted with Ψ-RNA, their binding affinity was in the high micromolar range and thus required optimization in view of therapeutic applications.[1] Herein, we describe the selection and functional analysis of an optimized peptide variant, *psi-pepB*, that shows antiviral activity in cell culture.

Results and Discussion

Peptide optimization on solid-support peptide arrays

To optimize the peptide ligands based on the previously identified consensus peptide HWWPWW (*psi-pepA*), we used peptide arrays on membrane supports for screening.[1,15,16] This method has been widely applied for epitope mapping and the identification of protein–protein interaction sites and to investigate peptide–DNA interactions.[17] To our knowledge, this is the first study adapting this method for peptide–RNA interactions. The experimental setup is illustrated in Figure 2a. Peptide arrays of permutations of the peptide GGSGSHWWPWWGGSG (parental sequence underlined) with one position each exchanged against all other 19 natural amino acids were probed with either the complete Ψ-RNA or a control RNA of the same length. Strikingly, only peptides containing either an arginine or lysine at any of the positions within the peptide HWWPWW specifically interacted with Ψ-RNA whereas interaction with ccr5 control RNA was below the detection limit (Figure 2b and Table 1). The peptide HKWPWW (*psi-pepB*) was selected for further analysis based on its solubility and binding characteristics for Ψ-RNA.

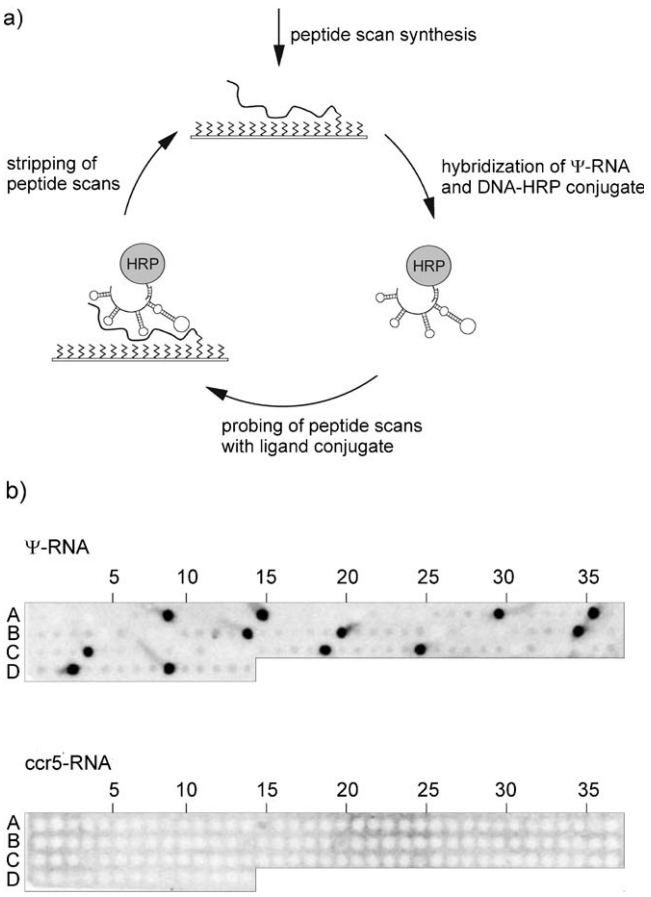

Figure 2. HIV-1 Ψ-RNA binding to peptide arrays. a) Scheme of the peptide optimization on membrane supports. b) Arrays of permutations of the peptide GGSGSHWWPWWGGSG (target residues underlined) were probed with Ψ-RNA and ccr5-RNA. Bound RNA was visualized by chemiluminescence imaging. The parental peptide GGSGSHWWPWWGGSG was included in each set of permutations (line 1: spot 7; line 2: spots 3, 24; line 3: spots 2, 29; line 4: spot 13).[1]

Table 1. Novel peptide ligands of HIV-1 Ψ-RNA.[a]

Line	Spot	Sequence
1	9	GGSGS**K**WWPWWGGSG
	15	GGSGS**R**WWPWWGGSG
	30	GGSGSH**K**WPWWGGSG
	36	GGSGSH**R**WPWWGGSG
2	14	GGSGSHW**K**PWWGGSG
	20	GGSGSHW**R**PWWGGSG
	35	GGSGSHWW**K**WWGGSG
3	4	GGSGSHWW**R**WWGGSG
	19	GGSGSHWWP**K**WGGSG
	25	GGSGSHWWP**R**WGGSG
4	3	GGSGSHWWPW**K**GGSG
	9	GGSGSHWWPW**R**GGSG

[a] Peptide sequences specifically recognized by Ψ-RNA are listed. The positions of the peptide spots depicted from Figure 2b are annotated, amino acids exchanged are given in bold. Sequences derived from the consensus peptide HWWPWW identified previously are underlined.[1]

Binding characteristics of *psi-pepB* to SL3-RNA

The binding of *psi-pepB* to SL3 was characterized by tryptophan fluorescence quenching (Figure 3a). At saturating concentrations, the interaction between SL3 and *psi-pepB* resulted in 60% reduction of the tryptophan fluorescence. This quenching was significantly higher than that previously observed with PBS and TAR sequences.[18] As fluorescence quenching results mainly from the π-π stacking of the tryptophan residues with the oligonucleotide bases, this suggests that a large fraction of the tryptophan residues of *psi-pepB* was stacked with the bases of SL3. Extensive stacking would favor inhibition of NCp7 binding to SL3, as the stacking of W37 of NCp7 with guanines is a major driving force in the binding of NCp7 to its RNA substrates.[5,19,20] The number of *psi-pepB* binding sites on SL3 was found to be 3 ± 1 under the conditions used, giving an occluded binding site of about six nucleotides per peptide, close to that found for TAR.[18] Assuming that the binding sites are identical and noninteracting, we obtained an apparent dissociation constant for *psi-pepB* of 1.1 ± 0.4 μM derived from three experiments. This affinity is about one order of magnitude higher than that of *psi-pepA*, suggesting that the substitution of W2 by a lysine residue significantly stabilizes the complex.[1]

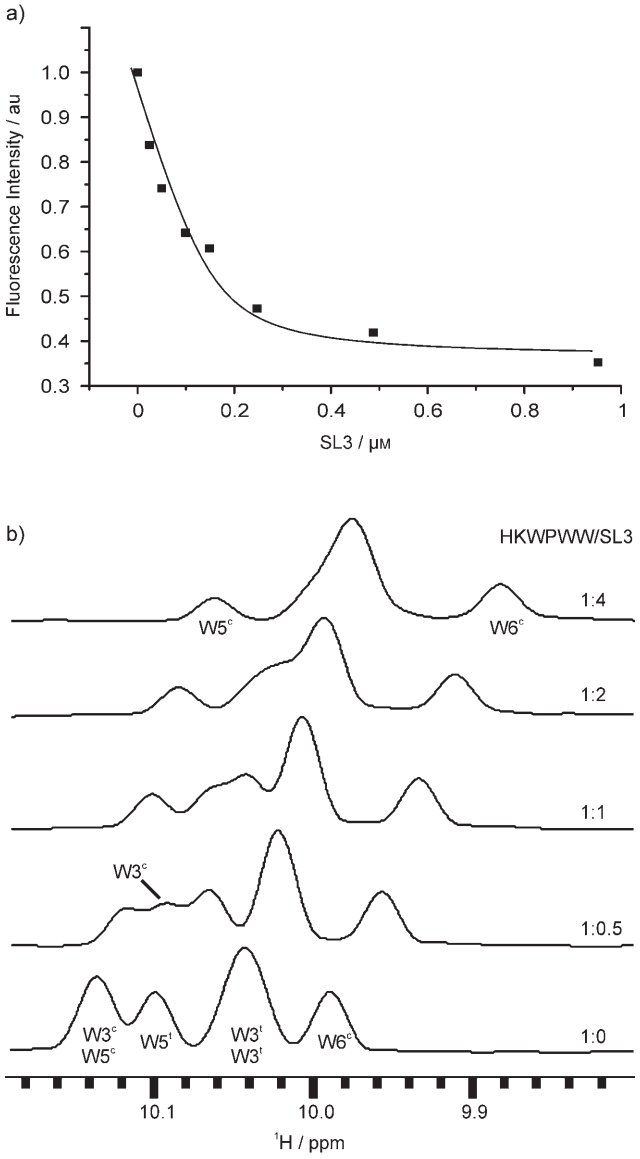

Figure 3. Binding of *psi-pepB* to SL3-RNA. a) Binding curve of HKWPWW-NH_2 with SL3-RNA. Excitation and emission wavelengths were 295 and 350 nm, respectively. The solid line represents the mathematical fit of the experimental points as described previously.[21] b) Titration of SL3-RNA to *psi-pepB*. One-dimensional ^{1}H NMR spectra of the peptide focusing on the tryptophan indole imino signals. The spectra correspond to the free *psi-pepB* and to *psi-pepB* after addition of SL3-RNA up to a fourfold excess. Each tryptophan residue results in two resonances, one resulting from the cis (c) and the other for the trans (t) conformation of proline.

As previously shown by NMR spectroscopy, *psi-pepB* adopted two global conformations with nearly equal populations depending on the cis/trans conformation of the peptide bond of the central proline.[18] By titrating SL3 up to a fourfold excess to a *psi-pepB* peptide solution followed by ^{1}H NMR analysis, distinctive shifts of the well-resolved tryptophan side chain imino proton resonances were observed for both conformations (Figure 3 b). All resonances shifted upfield and increased in line width (~30%) during the titration indicating an interaction of both conformations with the SL3 in the fast to intermediate NMR timescale. The largest shifts of the indole imino protons were observed for W5 in the *trans*-proline conformation and W3 in the *cis*-proline conformation. The conformational cis/trans equilibrium remained constant upon interaction with RNA. During the reverse titration of *psi-pepB* to SL3, no shifts of the imino resonances were detectable in the oligonucleotide base paired stem (data not shown). This assigns the specific binding region for the *psi-pepB* peptide to the GGAG tetraloop where no imino resonances are detectable. As *psi-pepB* also bound to the tetraloop of SL3 similar to the natural NCp7 ligand and due to its improved affinity, we expected that the peptide could inhibit HIV-1 replication.[5]

Antiviral activity of *psi-pepB*

We previously showed by ELISA that binding of *psi-pepA* to Ψ-RNA can be competed by Gagp55 and NCp7 underlining the specificity of binding for this RNA.[1] Herein, we assessed the capacity of the optimized peptide *psi-pepB* to inhibit HIV-1. The antiviral effect of *psi-pepB* was first analyzed by determining the transduction efficiencies of lentiviral vectors (LV) encoding the green fluorescence marker gene (gfp) in the presence of *psi-pepB* or control peptides by FACS analysis.[21] Expression of *psi-pepB* in cells was achieved upon transfection of a plasmid encoding the peptide sequence as a fusion with the marker gene for the red fluorescence protein (RFP). Transduction efficiencies of viral supernatants were then determined for different amounts of transfected RFP constructs in comparison with viruses generated in the presence of a control peptide (GSGSGS-RFP) or RFP alone. A representative experiment is shown in Figure 4. A clear reduction in LV transduction efficiencies was observed with increasing concentrations of transfected *psi-pepB* DNA. Whereas no reduction in LV titers was observed for the control peptide or RFP alone, *psi-pepB* expression reduced titers up to 85% in cells transfected with 1 μg of the corresponding DNA construct. However, the total amount of Gag proteins in transfected cells was comparable in the cell lysates as analyzed by Western blot analysis (data not shown).

Reduced LV titers were not due to toxicity of the peptides in the producer cells as determined by counting viable cells

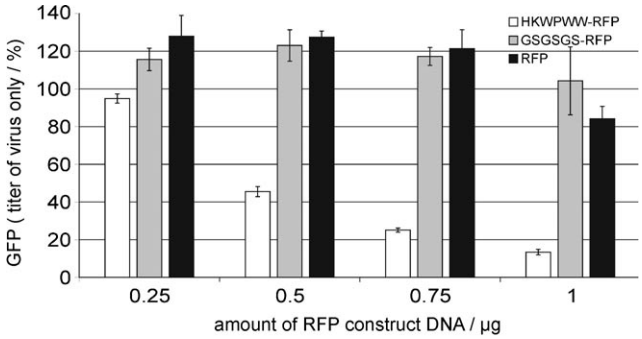

Figure 4. Antiviral activity of the optimized *psi-pepB* peptide on replication incompetent lentiviral particles. Transduction efficiencies of lentiviral particles produced in the presence of *psi-pepB* (white), a control peptide (gray), or RFP alone (black) were evaluated by titering lentiviral supernatants on 293T cells based on determining the percentage of GFP-positive cells by FACS analysis.

based on digital resistance determinations (data not shown). Furthermore, *psi-pepB* specifically inhibited the production of LV particles based on HIV-1 Ψ and Gag, whereas no specific inhibition was observed for γ-retroviral vectors containing the Ψ-signal and Gag of murine leukaemia virus (data not shown).

We next infected PM1 cells stably expressing the peptide-RFP-construct with HIV-1_{NL4-3} to confirm the antiviral activity of the *psi-pepB* peptide on replication-competent HIV-1. The amount of CAp24 antigen in culture supernatants was reduced by 70% at day five in the presence of *psi-pepB* (Supporting Information, SI Figure 1). Further, we analyzed the virus particles generated in the presence of *psi-pepB* or the control peptide by electron microscopy. Clearly, less budding viruses were observed in cells transduced with the *psi-pepB* peptide as compared to the control peptide and these viruses had a less condensed core (Figure 5). A detailed evaluation indeed revealed reduced virus production in *psi-pepB* expressing cells as compared to cells expressing the control peptide. This was observed at several levels (Supporting Information, SI Table 1): the mean number of virus producing cells (4.6 versus 3.5), the number of free virions per cell (21.0 versus 45.6), and the number of buddings (1.5 versus 2.1). The phenotype observed here is reminiscent of viruses with mutated Zn fingers in NCp7 that led to altered localization of Gag in the cells as well as impaired assembly and budding.[22]

To further prove that the antiviral activity is due to the *psi-pepB* peptide, we synthesized a rhodamine labeled *psi-pepB* peptide in conjunction with a protein transduction domain.[23] After delivery into cells infected with replication competent HIV-1_{LAI}, the antiviral effect was analyzed by titrating HIV-1 supernatants generated in the presence of *psi-pepB* or a control peptide on TZM-bl cells. *Psi-pepB* inhibited HIV-1_{LAI} by more than 90% after transduction of 2×40 μM of peptide, whereas the control peptide had only minimal effects (Figure 6). In these experiments, the first peptide addition was performed about 24 h after infection to circumvent a potential inhibitory effect of the peptides on reverse transcription, a process, which also depends on the chaperone activity of NCp7 during strand transfer reactions.[3,24] No toxic effects of the peptides were observed on P4.R5 or TZM-bl cells at any concentration tested (data not shown).

Interestingly, *psi-pepB* (HKWPWW) is highly homologous to short cationic antimicrobial peptides that disrupt large unilamellar vesicles.[25,26] As indolicidin (ILPW**KWPWW**PWRR) was previously shown to be virucidal against HIV-1 virions at a concentration of 174 μM after 60 min, we analyzed *psi-pepB* for potential additional virucidal activity after incubation with lentiviral particles.[25] At 35 μM, a concentration close to that showing 90% antiviral activity in our assays (40 μM, Figure 6), no virucidal activity of *psi-pepB* was found relative to the control peptide (Supporting Information, SI Figure 2). Thus, the antiviral activity observed in our assays is not due to virucidal activity. Virucidal activity on virions was only observed at much higher *psi-pepB* concentrations, being 35% at 174 μM relative to the control peptide. Therefore, virucidal activity is very unlikely to contribute significantly to the antiviral activity observed in our assays, in particular, as the cells were already infected with HIV-1 when the peptides were added.

Taken together, *psi-pepB* represents a peptide with antiviral activity against HIV-1, causing a strong reduction in particle production. From this study and our previous analyses it seems very likely that the tryptophan-rich peptide *psi-pepB* may mimic the hydrophobic platform of NCp7 that is essential for several functions.[18] These include the two strand transfer reactions during reverse transcription by binding to PBS and TAR sequences and RNA packaging by interaction with the Ψ-RNA. In line with this, *psi-pepB*, although originally selected with Ψ-RNA structures, also binds to sequences derived from PBS and TAR.[18] Thus, the antiviral activity observed here may result from the combined inhibitory effects at multiple steps during HIV-1 replication, where the action of NCp7 is needed. Based on the intriguing findings described here, the molecular details underlying the inhibitory action of the *psi-pepB* peptide at possibly more than one target have to be elucidated in further studies.

Experimental Section

Spot synthesis peptide membranes. Libraries of cellulose-bound peptides were synthesized by Fmoc-chemistry semiautomatically on a spot robot (ASP222, Intavis, Germany) as described previously.[15] Fmoc protected amino acids were obtained from Bachem, Switzerland. Peptide libraries were synthesized semiautomatically using Fmoc chemistry as separate spots on cellulose membranes carrying activated polyethylene glycol spacers.[15,16] To reduce steric hindrance for later RNA binding experiments, permutations of the peptide HWWPWW were synthesized in between an N-terminal GGSGS- and a C-terminal GGSG-linker. In vitro transcribed Ψ-RNA of HIV-1 was hybridized to an oligonucleotide complementary to the 5′ end (5′-CGAGAAUUACCCUCACUAAAGG-3′) coupled with horseradish peroxidase (HRP). The Ψ-RNA or the control ccr5-RNA (8.5 pmol) was hybridized with the HRP/DNA conjugate (20 pmol) in 10 μL at 45 °C for 1 h. Peptide scans were preincubated with Ψ-buffer (0.1 mM KCl, 5 mM HEPES, pH 7.4) and then saturated for 1 h with 2% blocking reagent (Roche, Germany) in blocking buffer (100 mM maleic acid, 150 mM NaCl, pH 7.5). Membranes were probed with the Ψ-RNA/DNA/HRP-hybrid for 2 h in Ψ-buffer (10 mL). After washing, bound RNA was visualized by chemiluminescence imaging. Membranes were reused after stripping using a three-step procedure: 1) incubation for 30 min with urea (8 M), SDS (20%), β-mercaptoethanol (0.1%), 2) incubation for 30 min with EDTA (10 mM), RNAse A (0.1 mg mL^{-1}), Tris/HCl (50 mM, pH 8), and 3) incubation for 5 min with trifluoroacetic acid.

Fluorescence titrations. Fluorescence titrations were performed on a thermostated Fluorolog spectrofluorometer (Jobin Yvon) by adding increasing SL3-RNA concentrations to *psi-pepB* (0.2 μM) in potassium phosphate buffer (100 mM, pH 6.5). The fluorescence intensity *I* at 350 nm was calculated as described previously and corrected for dilution, buffer fluorescence, and screening effects due to the oligonucleotide absorbance.[18]

^{1}H NMR Measurements. The titration of SL3-RNA to *psi-pepB* was monitored up to fourfold excess of RNA by 1D ^{1}H NMR on a Bruker 700 MHz spectrometer equipped with a ^{1}H, ^{13}C, ^{15}N triple resonance cryoprobe at 298 K. A 2D homonuclear NOESY spectrum was recorded at the final state to confirm the assignment. The peptide concentration was 0.2 mM in a buffer of potassium phosphate (25 mM) and potassium chloride (50 mM) at pH 6.2. All ex-

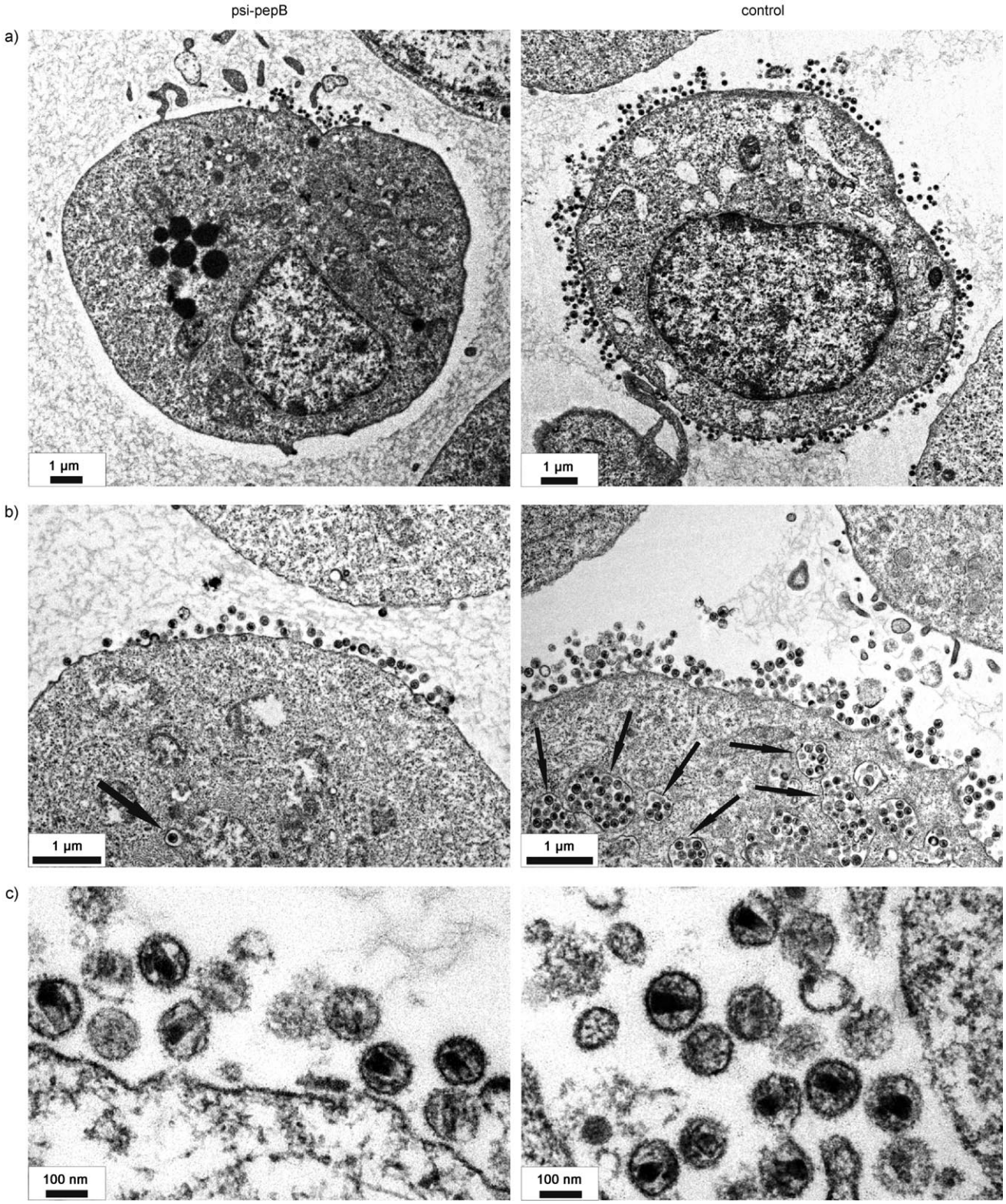

Figure 5. Electron microscopy of viral particles produced in cells expressing *psi-pepB* or control peptides. Effect of the *psi-pepB* peptide on synthesis and morphology of HIV-1 particles. Representative electron micrographs of infected PM1 cells stably expressing the HKWPWW peptide (left panel) or a control peptide (right panel). a) The expression of the peptide targeting the packaging signal leads to a significantly lower particle production and b) to a strongly reduced budding activity into the endosomal compartment (indicated by arrows). c) Mature HIV-1 cores of particles produced in the presence of the *psi-pepB* peptide appear more electron lucent and slightly less condensed.

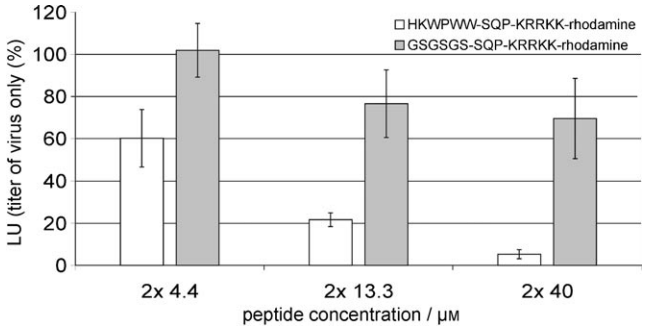

Figure 6. Antiviral activity of the optimized *psi-pepB* peptide linked to a protein transduction domain on replication competent HIV-1. Infection efficiencies of HIV-1_{LAI} virions generated in the presence of *psi-pepB* (white) or control peptide (gray) were analyzed by titering HIV-1_{LAI} supernatants on TZM-bl cells. The infected cells were grown for 44 h and the extent of infection was determined by measuring luciferase activity in the cell lysates.

periments were recorded with a jump-return-echo sequence, where the excitation maximum was centered on the chemical shift range of the tryptophan indole signals.

Cell lines. 293T, P4.R5 MAGI, and TZM-bl cells were maintained in DMEM supplemented with FCS (10%), penicillin (100 U mL^{-1}), 100 μg mL^{-1} streptomycin (100 μg mL^{-1}), and L-glutamine (2 mM) at 37 °C in a 5% CO_2 atmosphere.

Vector construction. For expression of peptides in mammalian cells, the plasmid pF25-GFP-Vpr kindly provided by Roland Stauber was modified.[27] The gfp gene was substituted by the rfp gene (Ds Red1) after PCR amplification from pHR'SINcPPT-SRW and cloning into the NheI/NarI sites. The vpr gene was deleted by restriction using NarI and XbaI and fill in with the Klenow fragment. A linker encoding the *psi-pepB* peptide or a GSGSGS control peptide was cloned upstream of rfp into the SacII/NheI sites to generate peptide-RFP fusion proteins.

Production of lentiviral particles. Replication defective lentiviral particles were generated by transient co-transfection of 293T cells with the plasmids pHR'SINcPPT-SEW, pCMVΔR8.91, and pMD2.VSVG by the calcium phosphate method.[21,28,29] For inhibition experiments, lentiviral particles were generated in the presence of the respective cotransfected pF25-peptide-RFP constructs. 293T cells were grown to 80% confluence and cotransfected with the three plasmids for lentivirus production (0.5 μg pHRSEWcPPT, 0.4 μg pCMVΔR8.91, and 0.9 μg pMD2.VSVG) and varying amounts of the pF25-peptide-RFP constructs. After 12 h, the supernatants were discarded and the cells were fed with fresh medium (2 mL). Viral stocks were harvested 48 h post transfection and filtered through 0.22 μm syringe filters before storage at −70 °C.

Transduction and determination of lentiviral titers. 293T cells were seeded at 1×10^5 cells and transduced with serially diluted viral vector stocks the next day in the presence of polybrene (8 μg mL^{-1}). Three days after transduction, cells were harvested, resuspended in PBS, and EGFP positive fluorescent cells were quantified by FACS analysis. The viral vector titer was determined as the percentage of EGFP positive cells multiplied by a factor to account for the dilution of the viral stock and total cell number.

Electron microscopy. PM1 cells stably expressing *psi-pepB* peptide or a control peptide in fusion with RFP were infected with HIV-1_{NL4-3} (MOI of 0.006), fixed at day five post infection with glutaraldehyde (2.5%) in HEPES (0.05 M), pH 7.2, and embedded in low melting point agarose (3%). The cells were postfixed with 1% osmium tetroxide, treated with 0.1% tannic acid (0.1%), and contrasted with uranyl acetate (2%). After dehydration the pellets were finally embedded in epoxy resin (Epon). Ultrathin sections were poststained with 2% uranyl acetate (2%) and lead citrate (0.1%) and were examined with a Tecnai Spirit transmission electron microscope (FEI Co., USA) at 120 keV. Images were taken with a Megaview III (Olympus Soft Imaging Solutions) camera. For each single infection, 25 complete cross sections of HIV-1 producing cells were analyzed.

Peptide synthesis. For synthesis of the rhodamine-labeled peptides Ac-HKWPWWSQPKRRKK and Ac-GSGSGSSQPKRRKK, an *N*-α-Fmoc-Lys(Mtt)-Wang resin was used. After removal of the lysine side-chain protecting group (4-Methyltitryl) with TFA (1%), TIS (5%), DCM (94%), and attachment of the dye 5(6)-Carboxytetramethyl-rhodamine (Novabiochem, Switzerland) to the free lysine side-chain amino group, this resin was used in automatic peptide synthesis on an ABI433A peptide synthesizer as previously described.[1]

Anti-HIV assays with the transduced peptides. P4.R5 MAGI cells were seeded at 1×10^4 cells and infected with HIV-1_{LAI} (MOI of 0.5). The next day (24 h after infection), the virus was washed off and rhodamine-labeled peptides were added to the cells in fresh medium for 24 h. Thereafter, the same amount of peptides was added again for a further 24 h until the supernatants were harvested. The viral titer of the preparations was determined on TZM-bl cells expressing firefly luciferase under the control of the HIV-1 LTR. 1×10^4 TZM-bl cells were seeded and infected with the viral supernatants in the presence of polybrene (8 μg mL^{-1}) for 44 h. The viral titer was quantified by luciferase assay. Cells were washed with PBS, lysed with harvest buffer (0.5 M Mes-Tris, 1 M DTT, 10% Triton-X-100 and glycerol), and light emission was measured on a Lumistar Galaxy Luminometer (BMG Labbiotechnologies, Germany).

Toxicity and virucidal activity assays. The viability of 293T cells transfected with the different peptide encoding plasmids was assessed by measuring resistance based on digital pulse processing. Briefly, transfected cells were harvested 48 h post transfection, resuspended in PBS, and viable cells were counted in an automated cell counting system (CasyTT, Schärfe Systems). Viability of peptide treated P4.R5 MAGI or TZM-bl cells was determined by the ViaLight kit (Cambrex) based on the luminometric measurement of ATP.

To assess the virolytic activity of the peptides on lentiviral particles, culture supernatants (10 μL) of producer cells (see production of lentiviral particles) were incubated with an equal volume of peptide solutions (0–174 μM) for 60 min at 37 °C in duplicates. After diluting 1:200 in growth medium, transduction efficiencies were determined on 293T cells as described above.

Acknowledgements

This work was supported by the Deutsche Forschungsgemeinschaft (SFB 579), the EU Integrated Project TRIoH (LSHB-CT-2003-503480) and the state of Hessen (Center of Biomolecular Magnetic Resonance). We thank Michaela Stoll and Hana Kunkel for expert technical assistance. We particularly thank Jean-Luc Darlix (Lyon) for helpful discussions. The following reagents were obtained through theNIH AIDS Research and Reference Reagent Program, Division of AIDS, NIAID, NIH: TZM-bl, P4.R5 MAGI, HIV-1_{LAI}, HIV-1_{NL4-3}. The authors declare that they have no competing financial interests.

Keywords: antiviral peptides · HIV-1 · NMR spectroscopy · RNA packaging · spot synthesis

[1] A. Pustowka, J. Dietz, J. Ferner, M. Baumann, M. Landersz, C. Konigs, H. Schwalbe, U. Dietrich, *ChemBioChem* **2003**, *4*, 1093–1097.
[2] J. L. Darlix, J. L. Garrido, N. Morellet, Y. Mely, H. De Rocquigny, *Adv. Pharmacol.* **2007**, *55*, 299–346.
[3] J. L. Darlix, M. Lapadat-Tapolsky, H. de Rocquigny, B. P. Roques, *J. Mol. Biol.* **1995**, *254*, 523–537.
[4] G. K. Amarasinghe, R. N. De Guzman, R. B. Turner, K. J. Chancellor, Z. R. Wu, M. F. Summers, *J. Mol. Biol.* **2000**, *301*, 491–511.
[5] R. N. De Guzman, Z. R. Wu, C. C. Stalling, L. Pappalardo, P. N. Borer, M. F. Summers, *Science* **1998**, *279*, 384–388.
[6] S. Campbell, V. M. Vogt, *J. Virol.* **1995**, *69*, 6487–6497.
[7] W. G. Rice, J. G. Supko, L. Malspeis, R. W. Buckheit, Jr., D. Clanton, M. Bu, L. Graham, C. A. Schaeffer, J. A. Turpin, J. Domagala, R. Gogliotti, J. P. Bader, S. M. Halliday, L. Coren, R. C. Sowder II, L. O. Arthur, L. E. Henderson, *Science* **1995**, *270*, 1194–1197.
[8] D. R. Chadwick, A. M. Lever, *Gene Ther.* **2000**, *7*, 1362–1368.
[9] H. De Rocquigny, V. Shvadchak, S. Avilov, C. Z. Dong, U. Dietrich, J. L. Darlix, Y. Mely, *Minirev. Med. Chem.* **2008**, *8*, 24–35.
[10] N. M. Dorman, A. M. Lever, *Gene Ther.* **2001**, *8*, 157–165.
[11] L. M. Miller Jenkins, J. C. Byrd, T. Hara, P. Srivastava, S. J. Mazur, S. J. Stahl, J. K. Inman, E. Appella, J. G. Omichinski, P. Legault, *J. Med. Chem.* **2005**, *48*, 2847–2858.
[12] J. C. Paillart, M. Shehu-Xhilaga, R. Marquet, J. Mak, *Nat. Rev. Microbiol.* **2004**, *2*, 461–472.
[13] E. Skripkin, J. C. Paillart, R. Marquet, M. Blumenfeld, B. Ehresmann, C. Ehresmann, *J. Biol. Chem.* **1996**, *271*, 28812–28817.
[14] M. Y. Park, J. Kwon, S. Lee, J. You, H. Myung, *Virus Res.* **2004**, *106*, 77–81.
[15] R. Frank, *Tetrahedron* **1992**, *48*, 9217–9232.
[16] J. Koch, M. Mahler, *Peptide Arrays on Membrane Supports*, Springer, Heidelberg, **2002**.
[17] M. Reuter, J. Schneider-Mergener, D. Kupper, A. Meisel, P. Mackeldanz, D. H. Kruger, C. Schroeder, *J. Biol. Chem.* **1999**, *274*, 5213–5221.
[18] C. Raja, J. Ferner, U. Dietrich, S. Avilov, D. Ficheux, J. L. Darlix, H. de Rocquigny, H. Schwalbe, Y. Mely, *Biochemistry* **2006**, *45*, 9254–9265.
[19] G. K. Amarasinghe, R. N. De Guzman, R. B. Turner, M. F. Summers, *J. Mol. Biol.* **2000**, *299*, 145–156.
[20] E. Bombarda, A. Ababou, C. Vuilleumier, D. Gerard, B. P. Roques, E. Piemont, Y. Mely, *Biophys. J.* **1999**, *76*, 1561–1570.
[21] L. Naldini, U. Blomer, P. Gallay, D. Ory, R. Mulligan, F. H. Gage, I. M. Verma, D. Trono, *Science* **1996**, *272*, 263–267.
[22] B. Grigorov, D. Decimo, F. Smagulova, C. Pechoux, M. Mougel, D. Muriaux, J. L. Darlix, *Retrovirology* **2007**, *4*, 54.
[23] M. C. Morris, J. Depollier, J. Mery, F. Heitz, G. Divita, *Nat. Biotechnol.* **2001**, *19*, 1173–1176.
[24] C. Bampi, S. Jacquenet, D. Lener, D. Decimo, J. L. Darlix, *Int. J. Biochem. Cell Biol.* **2004**, *36*, 1668–1686.
[25] W. E. Robinson, Jr., B. McDougall, D. Tran, M. E. Selsted, *J. Leukocyte Biol.* **1998**, *63*, 94–100.
[26] D. J. Schibli, R. F. Epand, H. J. Vogel, R. M. Epand, *Biochem. Cell Biol.* **2002**, *80*, 667–677.
[27] R. H. Stauber, S. Rulong, G. Palm, N. I. Tarasova, *Biochem. Biophys. Res. Commun.* **1999**, *258*, 695–702.
[28] C. Demaison, K. Parsley, G. Brouns, M. Scherr, K. Battmer, C. Kinnon, M. Grez, A. J. Thrasher, *Hum. Gene Ther.* **2002**, *13*, 803–813.
[29] R. Zufferey, D. Nagy, R. J. Mandel, L. Naldini, D. Trono, *Nat. Biotechnol.* **1997**, *15*, 871–875.

Received: August 2, 2007
Revised: December 14, 2007
Published online on January 18, 2008

